

Wind loads on roof cladding and fixings

John Ginger and David Henderson

Cyclone Testing Station, School of Engineering, James Cook University, Townsville, Qld 4811

Introduction

Roof failures during windstorms are mainly caused by large external suction pressures at the roof edges combined with large positive internal pressures resulting from a breach in the windward wall which generate large net uplift loads. Wind damage investigations following cyclones which hit northern Australia in the 1970s, found that most thin gauge sheet metal roof failures were initiated by fatigue cracking at the cladding fastener and the subsequent disengagement of cladding.

Following research and extensive industry consultation, guidelines for evaluating building products for use in cyclone prone regions of Australia, TR440 (1983) were developed. According to these guidelines which were included in AS1170.2 (1989), the performance of roof cladding, its fixings and their supporting structural elements, which also includes the battens are evaluated by applying cyclic loads in the following sequence; 8000 cycles at $0-0.40 p_d$, 2000 cycles at $0-0.50 p_d$, 200 cycles at $0-0.65 p_d$ and 1 cycle at $0-1.0 p_d$, where p_d is the ultimate limit state net design pressure. The net pressure is calculated by combining external and internal pressures acting on the tributary area of interest. Generally, internal pressure generated due to a dominant opening is applied for systems in cyclonic regions. The requirement of applying cyclic loads on tributary areas supported by batten-truss connections, albeit usually with a smaller pressures than that applied to a cladding fastener, is frequently queried by roofing system designers.

Reardon et al (1999) carried out a structural assessment of the housing stock in Exmouth, a small township located within the most cyclone prone region in Western Australia, (Region D as per AS/NZS1170.2), after it was hit by cyclone Vance in 1999. Peak gust wind speeds during Vance were estimated at between 55 and 70 m/s in the sheltered and exposed parts of town respectively, less than the ultimate limit state design wind speed of 85 m/s. Fatigue failure at the cladding fasteners was not evident in Exmouth after cyclone Vance. This was partly attributed to improved design of new roofs to satisfy TR440 requirements, and the fact that the older roofs had been upgraded by installing cyclone washers and roofing screws to attach the cladding to battens. However, a number of roof failures at the batten-truss connection as shown in Figure 1, were found, where generally no attempt had been made to improve the batten to truss (or rafter) connection.

Typical domestic house roof systems in Australia have battens placed at about 1.0 m intervals attached to roof trusses placed up to 1.2 m apart. The roof cladding is screwed to the battens by fasteners at a spacing of 150 to 200 mm. Thin-gauge steel ($\sim 0.6\text{mm}$), "top-hat" battens are increasingly replacing the traditional 40 mm deep timber battens. In these systems, a cladding fastener takes wind loads acting on an area of about 0.2 m^2 , whilst the batten-truss connection bears wind loads acting on a roof tributary area of $1.0\text{ m} \times 1.2\text{ m}$, six times the area supported by a cladding fastener. As in the case of cladding fasteners, batten-truss connections near the ridge and eaves can experience large wind loads and are also susceptible to fatigue failure at loads smaller than the ultimate limit state design load. This is a cause for concern as significant damage to large parts of a roof could arise from such failures.

The characteristics of fluctuating pressures on cladding-fastener and batten-truss connection tributaries during a strong wind event are studied by analysing external, internal and net pressures on selected parts of a building, with the aim of deriving equivalent loading cycles. Importantly, the influence of internal pressure fluctuations resulting from a dominant opening are considered in the analysis.

Experiments and Method of Analysis

Pressure measurements obtained on the $13.7 (b) \times 9.1 (d) \times 4.0 (h)$ m full-scale Texas Tech building are analysed. The characteristics of pressures on $1.0\text{m} \times 0.2\text{m}$ Area A, and $1.0\text{m} \times 1.8\text{m}$ Area B representative of a cladding-fastener and a batten-truss connection respectively shown in Figure 2, are studied. The

external, internal and net pressure fluctuations acting on cladding-fastener (Area A) and batten-truss (Area B) tributaries for approach wind flow normal to the 9.1 m wall with a dominant windward wall window opening area of 0.8 m² (i.e. 2% of wall) over a period of 15 mins are analysed in this paper.

The variation of pressure (p) with time (t) (described by the pressure coefficient referenced to the mean dynamic pressure at the roof height, $C_p = p / \frac{1}{2} \rho \bar{U}^2$) are analysed to give the mean value over time $C_{\bar{p}}$, the standard deviation C_{op} , the maximum $C_{\bar{p}}$, and the minimum $C_{\bar{p}}$. A normalised pressure $g_p = (C_p - C_{\bar{p}}) / C_{op}$ is defined such that maximum and minimum, pressure peak factors are $g_{\bar{p}} = (C_{\bar{p}} - C_{\bar{p}}) / C_{op}$ and $g_{\bar{p}} = (C_{\bar{p}} - C_{\bar{p}}) / C_{op}$ respectively.

Ginger (2001) showed that the probability density function $p_f(g_p)$ of external and net pressure fluctuations on Area A and Area B are not of the Gaussian form of $p_f(g_p) = (1/\sqrt{2\pi}) \exp^{-g_p^2/2}$, but are negatively skewed. Ginger (2001) also showed that a greater proportion of the fluctuating pressure energy on the roof is contained at higher frequencies compared to the approach wind velocity fluctuations. The net pressure spectrum on the building envelope is influenced by the internal pressure fluctuations.

The rainflow count method described by Amzalag et al (1994) and refined by Xu et al (1996) for wind loading applications is used to determine the equivalent number of cycles over the observation time. This method also gives the mean value and the peak-to-peak range of each pressure cycle, and provides a count of cycles within nominated means and ranges.

Results and Discussion

A portion of the external, internal and net C_p measured on Areas A and B of the building with a 2% windward wall opening are shown in Figure 3. Table 1 gives the pressure coefficients and pressure peak factors obtained on areas A and B of the building, and peak C_{ps} derived from AS/NZS 1170.2. The effective AS/NZS 1170.2 peak external pressure coefficients were derived from $C_{\bar{p},\bar{p}} = C_{pe} \times K_l \times G_U^2$, where C_{pe} is the quasi-steady external pressure coefficient, and velocity gust factor, $G_U = (\bar{U}_{3s} / \bar{U})$ at roof height of the building is 1.75. The dimension 'a' used in calculating the local pressure factor, K_l is 1.82m. The net uplift $C_{\bar{p}}$ on Area A, exceeded values derived from AS/NZS 1170.2 but compared favourably on Area B.

Table 2 gives the number of loading cycles contained within specified means and ranges on Area A and Area B obtained by applying the rainflow method with the external and net pressures measured over 15 mins. These mean and ranges of the pressure cycles are presented as a ratio of the peak external and net suction pressure coefficients, $C_{\bar{p}}$ on the corresponding tributary area. The total number of external pressure cycles on Area A of 6726 is exceeded by 12% by the total number of external pressure cycles on Area B of 7534. The total number of net pressure cycles on Area A and B are 7811 and 7740 respectively. Increased spatial variation of pressures on Area B compared to Area A is considered to generate the larger number of cycles.

The distribution of the cycle counts are similar for each of the four pressure records, with about 95% of the cycles having a peak-to-peak range less than 10% of the peak (external or net suction) pressures. These cycle counts were obtained for a roof height mean wind speed of 8.5 m/s. The number of cycles are expected to vary approximately proportionally with wind speed.

Conclusions

The following conclusions are made from analysing pressure measurements on areas representative of a cladding-fastener and batten-truss tributary on the roof of the full-scale Texas Tech building.

- Large external suction and net uplift pressures were experienced on cladding fastener and batten-truss connection tributaries close to the windward edge, on the roof.
- The pressure fluctuations on cladding-fastener and batten-truss tributaries have similar characteristics. Ginger (2001) showed that the probability densities and spectral densities of the external and net pressures on Areas A and B were similar.
- The number of external and net pressure cycles (and their means and ranges) on cladding-fastener batten-truss tributaries were determined using the rainflow count method. The batten-truss tributary was subjected to a larger number of (smaller magnitude) external and net pressure cycles compared with the cladding-fastener tributary.

References

- Amzallag, C., Gerey, J. P., Robert, J. L. and Bahuau, J., (1994) "Standardization of the Rainflow Counting Method for Fatigue Analysis", *Fatigue* Vol 16, 287-293.
- Australian Standard SAA Loading Code Part 2 Wind Loads AS1170.2 1989.
- Ginger, J. D. (2001), "Characteristics of wind loads on roof cladding and fixings" *Wind and Structures – An International Journal*, Vol. 4, No. 1 73-84.
- Reardon, G. F., Henderson, D. J. and Ginger, J. D. (1999), "A structural assessment of the effects of cyclone Vance on houses in Exmouth WA", *Cyclone Structural Testing Station, James Cook University, Technical Report No. 48*.
- Technical Record 440 (1983), "Guidelines for the testing and evaluation of products for cyclone-prone areas (TR 440)", Experimental Building Station, Department of Hosing and Construction.
- Xu, Y. L., Reardon, G., Mahlberg, J., Henderson, D. (1996), "Comparison of wind pressure and fatigue damage to hip and gable roof claddings", *Cyclone Structural Testing Station, James Cook University, Technical Report No. 43*.

Table 1. Pressure coefficients and pressure peak factors on the Texas Tech full-scale building

Tributary	Area, m ²	$C_{\bar{p}}$	$C_{\bar{p}}$	$C_{\bar{p}}$	C_{σ_p}	$g_{\bar{p}}$	$g_{\bar{p}}$	K_t	$C_{\bar{p},\bar{p}}$
Internal		0.65	2.80	-0.24	0.40	5.37	-2.23		2.14
A	0.2 (0.06a ²)	-1.43	-0.28	-7.10	0.60	1.93	-9.52	2.0	-5.51
B	1.8 (0.54a ²)	-1.37	-0.31	-4.50	0.54	1.99	-5.81	1.74	-4.82
A Net	0.2 (0.06a ²)	-2.08	-0.34	-8.36	0.88	1.97	-7.14		-7.65
B Net	1.8 (0.54a ²)	-2.02	-0.35	-6.36	0.84	1.97	-5.14		-6.96

* Velocity gust factor G_U at roof height = 1.75 'a' = minimum of (0.2b, 0.2d, h) = 1.82m

Table 2 Distribution of external and net pressure cycles on Areas A and B

Area A External Cps											Area A Net Cps											
Range	6.39	5.68	4.97	4.26	3.55	2.84	2.13	1.42	0.71	0	Range	7.52	6.69	5.85	5.02	4.18	3.34	2.51	1.67	0.84	0	
Mean	7.10	6.39	5.68	4.97	4.26	3.55	2.84	2.13	1.42	0.71	Mean	8.36	7.52	6.69	5.85	5.02	4.18	3.34	2.51	1.67	0.84	
0	-0.71	0	-0.84
-0.71	-1.42	466	-0.84	-1.67	295
-1.42	-2.13	1	44	3627	-1.67	-2.51	1	20	3062	
-2.13	-2.84	1	11	24	86	1817	-2.51	-3.34	2	7	23	73	2690	
-2.84	-3.55	.	.	.	4	1	5	10	48	440	-3.34	-4.18	.	.	1	2	5	6	10	56	1010	
-3.55	-4.26	.	.	.	2	.	4	.	11	91	-4.18	-5.02	.	.	1	1	2	4	10	21	359	
-4.26	-4.97	1	1	6	24	-5.02	-5.85	1	.	1	.	2	3	13	117		
-4.97	-5.68	-5.85	-6.69	10	
-5.68	-6.39	1	-6.69	-7.52	3	
-6.39	-7.10	-7.52	-8.36	
TOTAL	1	0	0	2	4	2	20	36	195	6466	TOTAL	1	0	1	3	2	9	19	47	183	7546	

Area B External Cps											Area B Net Cps												
Range	4.05	3.60	3.15	2.70	2.25	1.80	1.35	0.90	0.45	0	Range	5.72	5.09	4.45	3.82	3.18	2.54	1.91	1.27	0.64	0.00		
	4.50	4.05	3.60	3.15	2.70	2.25	1.80	1.35	0.90	0.45		6.36	5.72	5.09	4.45	3.82	3.18	2.54	1.91	1.27	0.64		
Mean											Mean												
0.0	-0.45	0.0	-0.64		
-0.45	-0.90	43	-0.64	-1.27	120		
-0.90	-1.35	11	1633	-1.27	-1.91	9	1598		
-1.35	-1.80	1	11	57	2958	-1.91	-2.54	2	8	57	2680			
-1.80	-2.25	.	.	.	2	5	6	25	95	1629	-2.54	-3.18	.	.	1	2	5	10	26	67	1779		
-2.25	-2.70	.	.	1	2	1	3	21	58	550	-3.18	-3.82	.	.	1	1	2	5	11	39	759		
-2.70	-3.15	1	1	.	1	1	2	4	9	33	225	-3.82	-4.45	1	1	.	2	1	3	5	10	24	277
-3.15	-3.60	1	.	3	19	80	-4.45	-5.09	2	6	16	146	
-3.60	-4.05	1	9	23	-5.09	-5.72	1	5	54	
-4.05	-4.50	1	1	7	-5.72	-6.36	3	
TOTAL	1	1	1	1	5	9	14	71	283	7148	TOTAL	1	1	1	4	4	10	24	62	217	7416		

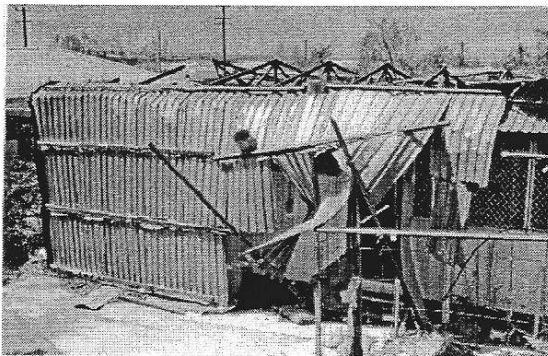


Figure 1. Failure of roof at the batten-truss connection during cyclone Vance in Exmouth.

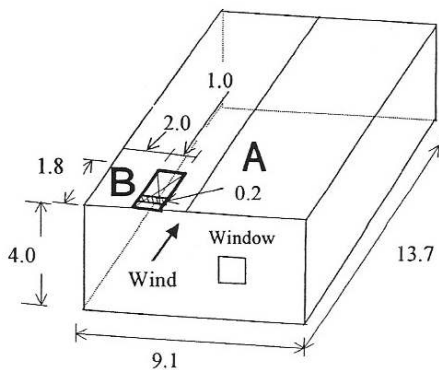


Figure 2. 13.7 × 9.1 × 4.0 m full-scale Texas Tech building showing cladding-fastener tributary area A (1.0 × 0.2 m²) and batten-truss tributary area B (1.0 × 1.8 m²)

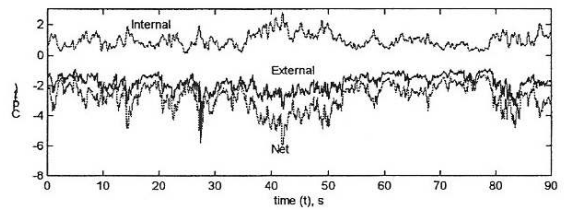
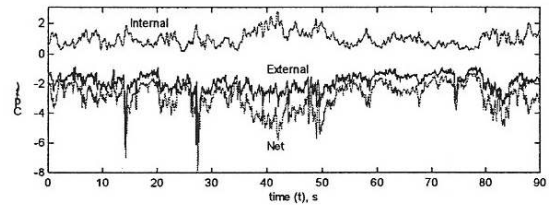


Figure 3. Part of internal, external and net Cp vs time on areas A and B, Texas Tech building